

Soft mode behavior in SrTiO₃/DyScO₃ thin films: Evidence of ferroelectric and antiferrodistortive phase transitions

D. Nuzhnyy,^{1,a)} J. Petzelt,¹ S. Kamba,¹ P. Kužel,¹ C. Kadlec,¹ V. Bovtun,¹ M. Kempa,¹ J. Schubert,² C. M. Brooks,^{3,4} and D. G. Schlom^{3,4}

¹Institute of Physics ASCR, Na Slovance 2, 182 21 Praha 8, Czech Republic

²Institute of Bio and Nanosystems and JARA-Fundamentals of Future Information Technology, Research Center Jülich, D-52425 Jülich, Germany

³Department of Materials Science and Engineering, Cornell University, Ithaca, New York 14853-1501, USA

⁴Department of Materials Science and Engineering, Penn State University, University Park, Pennsylvania 16802-5005, USA

(Received 30 September 2009; accepted 11 November 2009; published online 7 December 2009)

Infrared reflectance, terahertz transmittance, and microwave resonance measurements show that SrTiO₃ films, strained by $\sim 1\%$ in biaxial tension by growing them on (110) DyScO₃ substrates, undergo a pronounced phonon softening near 270 K. This in-plane soft-mode drives the ferroelectric transition. The appearance of two new low-frequency modes and splitting of the high-frequency TO4 mode provide evidence of an antiferrodistortive phase below ~ 180 K. © 2009 American Institute of Physics. [doi:10.1063/1.3271179]

Biaxially strained epitaxial (001) SrTiO₃ (STO) films grown on (110) DyScO₃ (DSO) films have undergone intensive study since it was shown that they become ferroelectric in the vicinity of room temperature.¹ The progress achieved in studying strained ferroelectric films has been thoroughly reviewed.^{2–4} It is now clear that, in agreement with theoretical predictions,^{1,4–8} the ferroelectric transition temperatures and phase diagrams of ferroelectric and related perovskite films, are extremely sensitive to epitaxial strain. This enables extensive tailoring of their dielectric properties by choosing an appropriate substrate. It was shown that the shift of the ferroelectric transition up to near room temperature for (001) STO/DSO films grown by reactive molecular-beam epitaxy (MBE) is caused by in-plane tensile strains of $\sim 1\%$ in the films induced by the single crystal (110) DSO substrate¹ due to its larger in-plane lattice parameter of 3.946 Å (Ref. 9) compared with that of 3.905 Å for bulk STO. As in other perovskite ferroelectrics, it is expected that the ferroelectric phase transition should be soft-mode (SM) driven. Therefore the study of the temperature dependent phonon response is of eminent interest.

The phonon properties of epitaxially strained STO films have been studied by Fourier-transform infrared (FTIR) and time-domain terahertz spectroscopy.^{10–15} STO/BaTiO₃ superlattices have also been examined by Raman scattering (see Ref. 16 for a recent review). The terahertz-IR studies of STO films were performed using the following substrates: (0001) c-cut sapphire,^{13,15} (10 $\bar{1}2$) R-cut sapphire,¹⁷ NdGaO₃,¹⁴ (LaAlO₃)_{0.18}–(SrAl_{0.5}Ta_{0.5}O₃)_{0.82} (LSAT),¹⁶ and DSO.^{10–12} In the case of NdGaO₃ and LSAT substrates, the films experience in-plane compressive strain, which results in a strongly stiffened phonon response. Concerning STO/DSO films, to date only room-temperature terahertz data has been published.^{10,12} Compared with bulk STO, a much softer phonon response was revealed. In addition to SM, clear evidence of a central-mode (CM) type excitation below its response, absent in bulk STO, has been observed. Both modes

contribute strongly to the static dielectric constant (by ~ 3000) at room temperature.

The low-frequency dielectric properties in STO/DSO films that have been reported to date strongly indicate relaxor behavior.¹⁸ Therefore some doubt may still remain about the existence of a macroscopic ferroelectric transition in such films. Here we report spectroscopic evidence of successive SM driven ferroelectric and antiferrodistortive transitions in STO/DSO films, which strongly supports the appearance of macroscopic ferroelectricity in these films below ~ 260 K.

We investigated the temperature dependence of the in-plane terahertz-IR response of a 100 nm thick film (the same as the 1 \times 100A sample in Ref. 10) prepared by pulsed-laser deposition. These measurements were complemented by resonance dielectric measurements in the GHz range.¹⁹ In addition, a ~ 30 nm thick film deposited by MBE was studied by FTIR and microwave (MW) techniques for comparison. The structural perfection of the films was characterized by four-circle x-ray diffraction (XRD). For both films, out-of-plane θ - 2θ scans revealed phase-pure, epitaxial (001)-oriented STO films. Additional XRD scans revealed that the 30 nm thick film was commensurately strained to the underlying (110) DSO substrate, while the 100 nm film showed partial strain relaxation.

A time-domain terahertz spectrometer utilizing a femto-second Ti:sapphire laser was used to measure the complex transmittance spectra, from which the in-plane complex dielectric response was calculated.¹⁰ The FTIR specular near-normal reflectance measurements were performed using a Bruker IFS 113v spectrometer. The DSO substrates carrying the investigated films were subsequently polished down to a thickness of ~ 100 μm for MW measurements. These measurements, which make use of a TE_{01 δ} composite dielectric resonator technique, detect the averaged in-plane response.¹⁹ IR and terahertz spectra were taken in two polarizations E_{||}[110] and E_{||}[001] (with respect to the DSO substrate). In the latter polarization the substrate exhibits two strong polar phonons below 100 cm⁻¹ preventing us from establishing the SM parameters for this polarization. However, no large in-plane SM anisotropy (due to the slightly orthorhombic

^{a)}Electronic mail: nuzhnyj@fzu.cz.

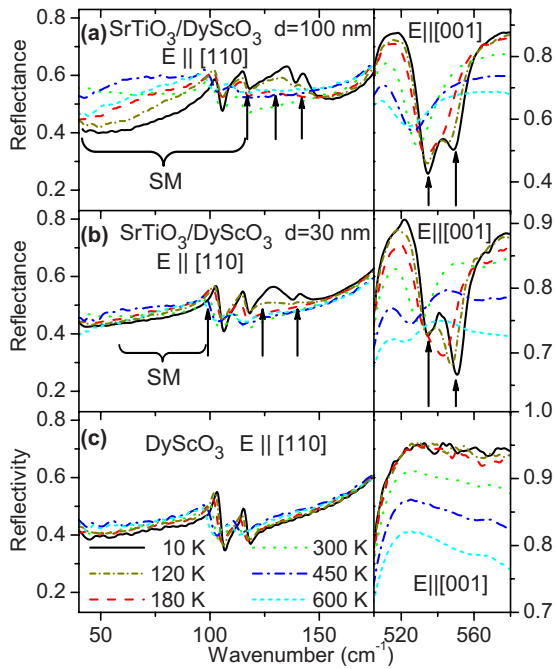


FIG. 1. (Color online) Polarized IR reflectance of (a) 100 nm and (b) 30 nm thick STO/DSO films and (c) polarized IR reflectivity of a bare (110) DSO substrate at the same temperatures. Only the low-frequency part of $E_{||[110]}$ spectra and high-frequency part of $E_{||[001]}$ spectra are shown. The fitted phonon mode frequencies at 10 K are marked by arrows.

DSO substrate) is expected. The observed in-plane low-frequency dielectric anisotropy of the films²⁰ is probably mainly related to the domain structure in the film. On the other hand, the parameters of the high-frequency TO4 mode could have been quantitatively retrieved only from the $E_{||[001]}$ polarization.

In Fig. 1 we show the $E_{||[110]}$ polarized FTIR reflectance below 175 cm^{-1} (SM region) for the two STO films at selected temperatures compared to that of a bare (110) DSO substrate. In the right part of Fig. 1 the high-frequency part of the $E_{||[001]}$ reflectance is presented, showing the TO4 mode region. Considering the opacity of the substrate, its reflectivity spectra were fitted with the factorized form of the dielectric function (see, e.g., Ref. 21). The resulting parameters of the substrate were used to fit the dielectric function of the film with a sum of independent harmonic oscillators formula (see, e.g., Ref. 13) using software for evaluation of the dielectric function of a two-slab (in general, multislabs) system.^{10,22} Fitting of the FTIR reflectance was performed simultaneously with the complex permittivity obtained from the terahertz data. The resulting dielectric functions below $\sim 250\text{ cm}^{-1}$ of the film are shown in Fig. 2. Above room temperature, where we have no terahertz data, the SM was fitted with a single heavily damped oscillator. Fitting the SM below room temperature, where we have terahertz data for the 100 nm film, was found to require an additional overdamped oscillator playing the role of CM, in agreement with prior studies,^{10,12} while for the thinner film the CM frequency could not be extracted from fitting the FTIR reflectance only. The resulting SM frequencies are plotted in Fig. 3(a). The error bars are shown for less accurate mode frequencies. Note the pronounced minimum in the 250–300 K region and strong phonon hardening and splitting below $\sim 180\text{ K}$. In Fig. 3(a) we also plotted the TO4 phonon fre-

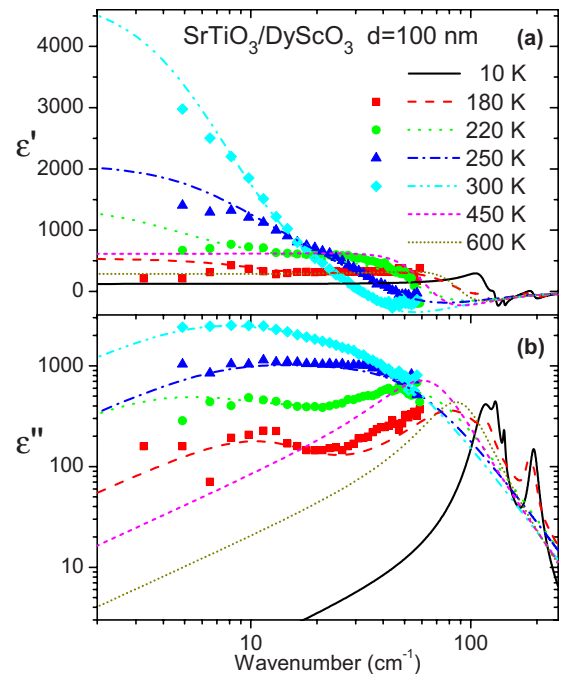


FIG. 2. (Color online) (a) Real and (b) imaginary part of the dielectric function (lines) of the 100 nm STO film obtained from fitting the IR reflectance along with the terahertz data (symbols).

quency obtained from a fit of the $E_{||[001]}$ polarized spectra, which splits clearly into two components in the same temperature range (Fig. 1). In bulk STO no similar splitting was observed.²³ The TO2 mode shows rather stiffened frequencies 193 and 205 cm^{-1} for $E_{||[110]}$ and $E_{||[001]}$ polarization at 10 K, respectively, compared with 172 cm^{-1} in the bulk.²³ Such large stiffening could partially result from bilin-

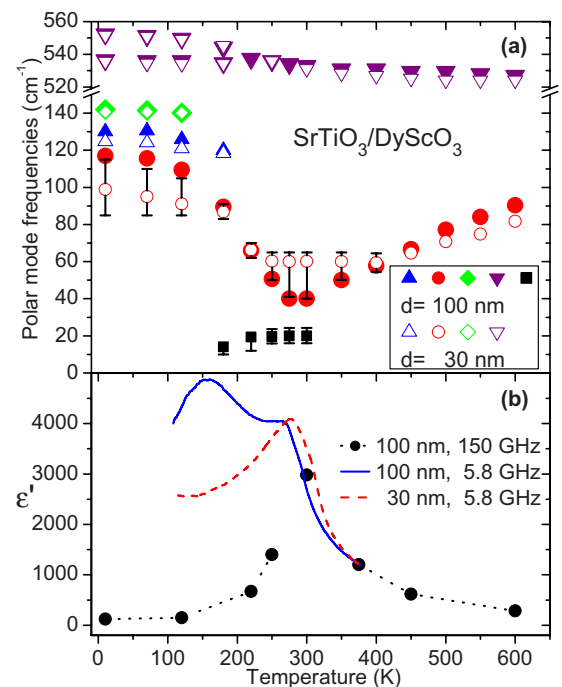


FIG. 3. (Color online) (a) Temperature dependence of the fitted low-frequency (from $E_{||[110]}$ polarization) and high-frequency (from $E_{||[001]}$ polarized IR spectra) polar modes in both STO films (open symbols – 30 nm, full symbols – 100 nm) and (b) temperature dependence of the dielectric function from the MW experiment for both STO films in comparison with the dielectric function in the subterahertz range.

ear coupling with the rather strong lower-frequency polar modes.

The minimum in the observed SM frequency corresponds well to the maximum in the MW and subterahertz permittivity near 270 K, as shown in Fig. 3(b). The MW permittivity of the 100 nm thick film shows, however, another maximum near 160 K. This maximum is absent in the terahertz data as well as in the MW permittivity of the thinner film [see Fig. 3(b)]. The difference between the terahertz and MW data below room temperature is caused mainly by domain-wall contributions to the permittivity, which cannot follow the terahertz frequencies. Moreover, the 100 nm thick film is partially structurally relaxed and therefore dielectrically inhomogeneous, which also may produce effective dielectric dispersions. Since the measured MW in-plane response is unpolarized and strongly influenced by domain-wall contributions and inhomogeneities, it might result in the appearance of a second maximum in the permittivity versus temperature of the thicker film. Above room temperature, the permittivities of both films obey the Curie–Weiss law with Curie temperatures of 250 and 276 K, respectively. Even though the accuracy of the absolute permittivity values from MW and terahertz data is rather low (roughly $\pm 30\%$), their relative temperature dependences are quite reliable and clearly indicate a SM driven ferroelectric transition in the 260–280 K region in both films. It should be stressed that such behavior differs from that of relaxor ferroelectrics in which no phonon softening is connected with the permittivity versus temperature maximum.²⁴

In both films new phonon peaks emerge below ~ 180 K in the 120–145 and 540 cm^{-1} range [Fig. 3(a)]. These peaks provide evidence for the antiferrodistortive transition of strained STO that is expected from theory;^{5,6} its possible existence was suggested from small anomalies observed in dielectric¹⁸ as well as second-harmonic generation measurements²⁵ at around 165 K in similar films. According to the theory, the tilt axis of the octahedral rotation in this phase should agree with the in-plane lying ferroelectric axis.⁶ An analogous effect in the SM region was also observed for a STO/(0001)-sapphire film.¹³ It was interpreted as the structural SM doublet from the R-point of the Brillouin zone activated by its linear coupling with the ferroelectric SM in a phase which is both ferroelectric and antiferrodistortive. We note that all three SMs in both STO/DSO films are strongly stiffened compared to their low-temperature behavior in bulk STO, where their frequencies at ~ 10 K are 8 and 17 cm^{-1} for the ferroelectric SM doublet²⁶ and 15 and 41 cm^{-1} for the structural SM doublet.²⁷ As in Ref. 13, we do not resolve the small ferroelectric TO1 SM splitting (but unlike Ref. 13 we see the TO4 mode splitting). Compared to bulk STO crystals, the structural SM splitting in our films is much smaller (~ 12 cm^{-1}), which indicates smaller in-plane anisotropy induced by the antiferrodistortive transition. Smaller splitting and consequently smaller tetragonality due to this transition was also observed in bulk STO ceramics.²³

In conclusion, we found unambiguous evidence of a SM driven in-plane ferroelectric transition, as well as a subsequent antiferrodistortive transition in epitaxial STO/DSO films. The temperatures of both phase transitions are influenced by the strain and are in a good agreement with theoretical predictions. We also determined the in-plane polar phonon behavior in such films for all three of their phases.

This work was supported by the Czech Project Nos. 202/09/0682, KJB100100704, A100100907, and AVOZ10100520, and the National Science Foundation through the MRSEC program (Grant No. DMR-0820404). We are grateful to R. Uecker, M. Bernhagen, and P. Reiche for providing us with the DyScO₃ substrates.

- ¹J. H. Haeni, P. Irvin, W. Chang, R. Uecker, P. Reiche, Y. L. Li, S. Choudhury, W. Tian, M. E. Hawley, B. Craigo, A. K. Tagantsev, X. Q. Pan, S. K. Streiffer, L. Q. Chen, S. W. KircVhoefer, J. Levy, and D. G. Schlom, *Nature (London)* **430**, 758 (2004).
- ²M. Dawber, K. M. Rabe, and J. F. Scott, *Rev. Mod. Phys.* **77**, 1083 (2005).
- ³N. Setter, D. Damjanovic L. Eng, G. Fox, S. Gevorgian, S. Hong, A. Kingon, H. Kohlstedt, N. Y. Park, G. B. Stephenson, I. Stoltichnov, A. K. Tagantsev, D. V. Taylor, and T. Yamada S. Streiffer *J. Appl. Phys.* **100**, 051606 (2006).
- ⁴D. G. Schlom, L.-Q. Chen, C. B. Eom, K. M. Rabe, S. K. Streiffer, and J.-M. Triscone, *Annu. Rev. Mater. Res.* **37**, 589 (2007).
- ⁵N. A. Pertsev, A. K. Tagantsev, and N. Setter, *Phys. Rev. B* **61**, R825 (2000); **65**, 219901(E) (2002).
- ⁶Y. L. Li, S. Choudhury, J. H. Haeni, M. D. Biegalski, A. Vasudevarao, A. Sharan, H. Z. Ma, J. Levy, V. Gopalan, S. Trolier-McKinstry, D. G. Schlom, Q. X. Via, and L. Q. Chen, *Phys. Rev. B* **73**, 184112 (2006).
- ⁷A. Antons, J. B. Neaton, K. M. Rabe, and D. Vanderbilt, *Phys. Rev. B* **71**, 024102 (2005).
- ⁸V. B. Shirokov, Yu. I. Yuzyuk, B. Dkhil, and V. V. Lemanov, *Phys. Rev. B* **79**, 144118 (2009).
- ⁹B. Veličkov, V. Kahlenberg, R. Bertram, and M. Bernhagen, *Z. Kristallogr.* **222**, 466 (2007).
- ¹⁰P. Kužel, F. Kadlec, J. Petzelt, J. Schubert, and G. Panaitov, *Appl. Phys. Lett.* **91**, 232911 (2007).
- ¹¹P. Kužel, C. Kadlec, F. Kadlec, J. Schubert, and G. Panaitov, *Appl. Phys. Lett.* **93**, 052910 (2008).
- ¹²C. Kadlec, F. Kadlec, H. Němec, P. Kužel, J. Schubert, and G. Panaitov, *J. Phys.: Condens. Matter* **21**, 115902 (2009).
- ¹³T. Ostapchuk, J. Petzelt, V. Železný, A. Pashkin, J. Pokorný, I. Drbohlav, R. Kužel, D. Rafaja, B. P. Gorshunov, M. Dressel, Ch. Ohly, S. Hoffmann-Eifert, and R. Waser *Phys. Rev. B* **66**, 235406 (2002).
- ¹⁴T. Yamada, J. Petzelt, A. K. Tagantsev, S. Denisov, D. Noujni, P. K. Petrov, A. Mackova, K. Fujito, T. Kiguchi, K. Shinozaki, N. Mizutani, V. O. Sherman, P. Mural, and N. Setter, *Phys. Rev. Lett.* **96**, 157602 (2006).
- ¹⁵D. Nuzhnyy, J. Petzelt, S. Kamba, T. Yamada, M. Tyunina, A. K. Tagantsev, J. Levoska, and N. Setter, *J. Electroceram.* **22**, 297 (2009).
- ¹⁶D. A. Tenne and X. Xi, *J. Am. Ceram. Soc.* **91**, 1820 (2008).
- ¹⁷P. Kužel, F. Kadlec, H. Němec, R. Ott, E. Hollmann, and N. Klein, *Appl. Phys. Lett.* **88**, 102901 (2006).
- ¹⁸M. D. Biegalski, Y. Jia, D. G. Schlom, S. Trolier-McKinstry, S. K. Streiffer, V. Sherman, R. Uecker, and P. Reiche, *Appl. Phys. Lett.* **88**, 192907 (2006).
- ¹⁹V. Bovtun, S. Veljko, A. Axelsson, S. Kamba, N. Alford, and J. Petzelt, *Integr. Ferroelectr.* **98**, 53 (2008).
- ²⁰M. D. Biegalski, E. Vlahos, G. Sheng, Y. L. Li, M. Bernhagen, P. Reiche, R. Uecker, S. K. Streiffer, L. Q. Chen, V. Gopalan, D. G. Schlom, and S. Trolier-McKinstry, *Phys. Rev. B* **79**, 224117 (2009).
- ²¹E. Buixaderas, S. Kamba, and J. Petzelt, *Ferroelectrics* **308**, 131 (2004).
- ²²J. Petzelt, P. Kužel, I. Rychetsky, A. Pashkin, and T. Ostapchuk, *Ferroelectrics* **288**, 169 (2003).
- ²³J. Petzelt, T. Ostapchuk, I. Gregora, I. Rychetský, S. Hoffmann-Eifert, A. V. Pronin, Y. Yuzyuk, B. P. Gorshunov, S. Kamba, V. Bovtun, J. Pokorný, M. Savinov, V. Porokhonsky, D. Rafaja, P. Vaněk, A. Almeida, M. R. Chaves, A. A. Volkov, M. Dressel, and R. Waser, *Phys. Rev. B* **64**, 184111 (2001).
- ²⁴J. Hlinka, J. Petzelt, S. Kamba, D. Noujni, and T. Ostapchuk, *Phase Transitions* **79**, 41 (2006).
- ²⁵A. Vasudevarao, A. Kumar, L. Tian, J. H. Haeni, Y. L. Li, C.-J. Eklund, Q. X. Jia, R. Uecker, P. Reiche, K. M. Rabe, L. Q. Chen, D. G. Schlom, and V. GopaVlan, *Phys. Rev. Lett.* **97**, 257602 (2006).
- ²⁶A. Yamanaka, M. Kataoka, Y. Inaba, K. Inoue, B. Hehlen, and E. Courtens, *Europhys. Lett.* **50**, 688 (2000).
- ²⁷P. A. Fleury, J. F. Scott, and J. M. Worlock, *Phys. Rev. Lett.* **21**, 16 (1968).